Small Molecule Therapeutics

Molecular Cancer Therapeutics

Selective Inhibition of EZH2 by EPZ-6438 Leads to Potent Antitumor Activity in *EZH2*-Mutant Non-Hodgkin Lymphoma

Sarah K. Knutson[1], Satoshi Kawano[3], Yukinori Minoshima[3], Natalie M. Warholic[1], Kuan-Chun Huang[2], Yonghong Xiao[1], Tadashi Kadowaki[2], Mai Uesugi[3], Galina Kuznetsov[2], Namita Kumar[2], Tim J. Wigle[1], Christine R. Klaus[1], Christina J. Allain[1], Alejandra Raimondi[1], Nigel J. Waters[1], Jesse J. Smith[1], Margaret Porter-Scott[1], Richard Chesworth[1], Mikel P. Moyer[1], Robert A. Copeland[1], Victoria M. Richon[1], Toshimitsu Uenaka[3], Roy M. Pollock[1], Kevin W. Kuntz[1], Akira Yokoi[3], and Heike Keilhack[1]

Abstract

Mutations within the catalytic domain of the histone methyltransferase EZH2 have been identified in subsets of patients with non-Hodgkin lymphoma (NHL). These genetic alterations are hypothesized to confer an oncogenic dependency on EZH2 enzymatic activity in these cancers. We have previously reported the discovery of EPZ005678 and EPZ-6438, potent and selective *S*-adenosyl-methionine-competitive small molecule inhibitors of EZH2. Although both compounds are similar with respect to their mechanism of action and selectivity, EPZ-6438 possesses superior potency and drug-like properties, including good oral bioavailability in animals. Here, we characterize the activity of EPZ-6438 in preclinical models of NHL. EPZ-6438 selectively inhibits intracellular lysine 27 of histone H3 (H3K27) methylation in a concentration- and time-dependent manner in both *EZH2* wild-type and mutant lymphoma cells. Inhibition of H3K27 trimethylation (H3K27Me3) leads to selective cell killing of human lymphoma cell lines bearing EZH2 catalytic domain point mutations. Treatment of *EZH2*-mutant NHL xenograft-bearing mice with EPZ-6438 causes dose-dependent tumor growth inhibition, including complete and sustained tumor regressions with correlative diminution of H3K27Me3 levels in tumors and selected normal tissues. Mice dosed orally with EPZ-6438 for 28 days remained tumor free for up to 63 days after stopping compound treatment in two *EZH2*-mutant xenograft models. These data confirm the dependency of *EZH2*-mutant NHL on EZH2 activity and portend the utility of EPZ-6438 as a potential treatment for these genetically defined cancers. *Mol Cancer Ther; 13(4); 842–54. ©2014 AACR.*

Introduction

Regulation of gene transcription by enzyme-catalyzed, covalent modification of histone proteins and nucleic acids is a critical biologic process (1). Posttranslational histone modifications that are known to contribute to the regulation of gene transcription include acetylation, methylation, phosphorylation, and ubiquitinylation (2). Methylation events at lysine and arginine residues, catalyzed by histone methyltransferases (HMT), have been subjected to intense investigations in recent years because HMTs represent a particularly attractive class of targets for drug discovery efforts, because of their disease association and druggability (3). For instance, genetic alterations have been identified in a number of HMTs in human cancers where they are purported to play a causal role in malignancies. In addition, selective small molecule HMT inhibitors have been demonstrated to cause context-specific antiproliferative activity in cancers bearing genetic alterations in the targeted HMT or related pathways.

EZH2 is the catalytic subunit of the multiprotein HMT complex known as polycomb repressive complex 2 (PRC2; refs. 4 and 5). EZH2 has been implicated in several cancer types by mutation, amplification, and/or overexpression (6). Heterozygous *EZH2* mutations within the catalytic SET domain have been observed in 10% of non-Hodgkin lymphomas (NHL) at 3 hotspots (Y646, A682, and A692, referring to *EZH2* variant NM_004456.3; refs. 7–9). Interestingly, these mutations are exclusively found in lymphomas of germinal center origin, in line with recent data

Authors' Affiliations: [1]Epizyme Inc., Cambridge; [2]Eisai Inc., Andover, Massachusetts; and [3]Eisai Co. Ltd., Tsukuba-shi, Ibaraki, Japan

Note: Supplementary data for this article are available at Molecular Cancer Therapeutics Online (http://mct.aacrjournals.org/).

S.K. Knutson and S. Kawano contributed equally to this work.

Current address for V.M. Richon: Sanofi, 270 Albany Street, Cambridge, MA 02139.

Corresponding Authors: Akira Yokoi, Eisai Co. Ltd., 5-1-3 Tokodai, Tsukuba-shi, Ibaraki, 300-2635, Japan. Phone: 81-29-847-5748; Fax: 81-29-847-2759; E-mail: a-yokoi@hhc.eisai.co.jp; and Heike Keilhack, Epizyme Inc., 400 Technology Square, 4th Floor, Cambridge, MA 02139. Phone: 617-500-0618; Fax: 617-349-0707; E-mail: hkeilhack@epizyme.com

doi: 10.1158/1535-7163.MCT-13-0773

suggesting a master role of EZH2 in B-cell germinal center formation and maintenance (10, 11). Mutant EZH2 proteins change their substrate specificity and act in concert with wild-type EZH2 to generate abnormally high levels of trimethylated lysine 27 on histone H3 (H3K27Me3), leading to abnormal repression of PRC2 targets, which drives lymphomagenesis (12–16). These preclinical data provide the basis for EZH2 inhibition as a specific rational therapy for germinal center–derived B-cell lymphomas, and we and others previously reported that selective inhibition of EZH2 in cell culture results in selective killing of lymphoma cells bearing *EZH2* mutations (17–20). EPZ-6438 is one of a several potent and selective EZH2 inhibitors that we and others have recently reported. These inhibitors, including our previously published tool compound EPZ005687, share similar *in vitro* properties (i.e., mechanism of action, specificity, and cellular activity) as EPZ-6438. However, EPZ-6438 is among the most potent EZH2 inhibitors described to date and demonstrates significantly improved pharmacokinetic properties relative to EPZ005687, including good oral bioavailability in animals. Consistent with this, we previously demonstrated that oral dosing of EPZ-6438 leads to potent *in vivo* target inhibition and antitumor activity in a *SMARCB1*-deleted malignant rhabdoid tumor xenograft model (21). Here we expand on the pharmacologic properties of EPZ-6438 and assessed whether *EZH2*-mutant lymphomas are selectively sensitive to EZH2 inhibition *in vitro* and *in vivo*, which would suggest its application as a novel targeted therapy in *EZH2* mutant–bearing NHL.

Materials and Methods

Synthesis of EPZ-6438

A synthetic route of EPZ-6438 is described in PCT patent application publication number WO/2012/142504.

Cell culture, immunoblot, and proliferation assays

Lymphoma cell lines OCI-LY19 (ACC-528), WSU-DLCL2 (ACC-575), KARPAS-422 (ACC-32), and SU-DHL-10 (ACC-576) were obtained from DSMZ. RL (CRL-2261), Toledo (CRL-2631), Pfeiffer (CRL-2632), SU-DHL-6 (CRL-2959), and Farage (CRL-2630) cells were obtained from American Type Culture Collection. DOHH2 (HTL99022) was obtained from BBCF. Toledo, SU-DHL-6, and KARPAS-422 cell lines were cultured in RPMI + 20% FBS, whereas all other cell lines were cultured in RPMI + 10% FBS. Cell lines were authenticated by STR assay and *EZH2* mutational status was verified by sequence analysis. Histone extractions, immunoblot, 11-day proliferation assays, methylation time course, cell cycle, and apoptosis experiments were performed as previously described (17).

High throughput proliferation assay

For the assessment of the effect of compounds on the proliferation of the WSU-DLCL2 cell line, exponentially growing cells were plated in 384-well white opaque plates at a density of 1,250 cells/mL in a final volume of 50 μL of assay medium (RPMI 1640 supplemented with 20% v/v heat-inactivated FBS, 100 units/mL penicillin–streptomycin). A compound source polypropylene 384-well plate with an assigned container number was prepared by performing triplicate 9-point 3-fold serial dilutions in dimethyl sulfoxide (DMSO), beginning at 10 mmol/L (final top concentration of compound in the assay was 20 μmol/L and the final concentration of DMSO was 0.2%). A 100-nL aliquot from the compound stock plate was added to its respective well in the cell plate. The 100% inhibition control consisted of cells treated with 200 nmol/L final concentration of staurosporine and the 0% inhibition control consisted of DMSO-treated cells. After addition of the compounds, assay plates were incubated for 6 days at 37°C, 5% CO_2, relative humidity >90%. Cell viability was measured by quantitation of ATP present in the cell cultures, by adding 35 μL of Cell Titer Glo reagent to the cell plates. Luminescence was read in the SpectraMax M5 instrument. The concentration inhibiting cell viability by 50% was determined using a 4-parametric fit of the normalized dose–response curves.

Chromatin immunoprecipitation followed by PCR (ChIP-PCR)

WSU-DLCL2 cells were treated with either DMSO or 1 μmol/L EPZ-6438 for 4 days. Cells were harvested and fixed according to published methods provided by Active Motif (http://www.activemotif.com/documents/1848.pdf). Antibodies used for ChIP include: EZH2 (Active Motif catalog no. 39901), SUZ12 (Abcam ab12073), and H3K27Me3 (CST 9733). Primer design and data analysis were performed by Active Motif using the ChIP-IT qPCR Analysis Kit published manual (catalog no. 53029).

Cell treatments for gene expression profiling, data processing, and further analyses

Each of the 4 cell lines (WSU-DLCL2, KARPAS-422, SU-DHL-6, and Pfeiffer) were plated in 6-well plates at an initial seeding density to ensure cell densities were within linear log phase growth for days 2 and 4 of the time course. Cells were treated with either DMSO, or 1× or 10× LCC concentration of EPZ-6438. EPZ-6438 LCC concentrations for each of the cell lines are as follows: WSU-DLCL2, 200 nmol/L; KARPAS-422, 100 nmol/L; SU-DHL-6, 200 nmol/L; and Pfeiffer, 0.5 nmol/L. At each time point, cells were harvested by centrifugation, washed with PBS, and cell pellets were snap frozen. A second set of cells were treated in a similar manner on day 0, counted on day 4, split back to the original plating density, and redosed with DMSO, 1× or 10× LCC concentration of EPZ-6438 for the day 6 time point. RNA extraction and amplification and subsequent microarray processing was performed by Expression Analysis, Inc. as previously described (17). Both normalized expression data and CEL files are deposited in GEO under GSE49284.

RNA extraction and amplification and subsequent microarray processing was performed by Expression

Analysis, Inc. as previously described (17). Normalized Affymetrix U133 plus2 array expression data were created for all samples from CEL files using the Expression File Creator Module from GenePattern (http://genepattern.broadinstitute.org). Quantile normalization and GCRMA were selected as the algorithms to generate normalized expression values. Both normalized expression data and CEL files are deposited in GEO under GSE49284.

Two sample *t* tests were carried out for differentially expressed genes upon EPZ-6438 treatment, for each cell line at 2 doses (LCC and 10× LCC) and 3 time points (2, 4, and 6 days). Genes with fold change >2 or <0.5 and *P*-value < 0.05 were further analyzed through the use of Ingenuity Pathway Analysis (Ingenuity Systems, www.ingenuity.com).

Gene set enrichment analysis (GSEA) was performed on EPZ-6438 versus DMSO-treated 2-sample comparison for all cell lines, each at 2 concentrations and 3 time points, using the GSEA Java-enabled desktop software (Version 2.0.13, http://www.broadinstitute.org/gsea/index.jsp). Probe sets were collapsed to gene symbols (HUGO nomenclature) using maximum probe intensity collapsing mode. Permutation was carried out on gene set, rather than phenotype, to accommodate small sample size. Customized KEGG pathway gene sets [added Ben-Porath embryonic stem (ES) cell and Velichutina Centroblast PRC2 target sets, as described (17)] as well as transcription factor binding motif gene sets from MSigDB version 4.0 (http://www.broadinstitute.org/gsea/msigdb/index.jsp) were used for all GSEA analyses.

Xenograft studies

All the procedures related to animal handling, care, and the treatment in this study were performed according to the guidelines approved by the Institutional Animal Care and Use Committee of CRL Piedmont, Eisai Tsukuba, and Eisai Andover following the guidance of the Association for Assessment and Accreditation of Laboratory Animal Care.

WSU-DLCL2 cells were harvested during mid-log phase growth, and resuspended in PBS with 50% Matrigel (BD Biosciences). SCID mice received 1×10^7 cells (0.2 mL cell suspension) subcutaneously in the right flank. After 10 to 30 days, mice with 108 to 126 mm^3 tumors were sorted into treatment groups with mean tumor volumes of 117 to 119 mm^3. EPZ-6438 or vehicle (0.5% NaCMC + 0.1% Tween-80 in water) was administered at the indicated doses on 3 times daily every 8 hours, 2 times a day every 12 hours, or once a day schedules for either 7 or 28 days by oral gavage. Each dose was delivered in a volume of 0.2 mL/20 g mouse (10 mL/kg), and adjusted for the last recorded weight of individual animals. The maximal treatment length was 28 days. On day 7 or day 28 during the studies, mice were sampled in a prespecified fashion. Sampling included nonterminal bleeds (0.25 mL) from the mandibular vein without anesthesia and full volume blood collection via terminal cardiac puncture under CO_2 anesthesia. Blood samples were processed for plasma, with K_2-EDTA as anticoagulant. The plasma samples were frozen at −80°C and stored before bioanalysis of compound levels. Tumors were harvested from specified mice under RNase-free conditions and bisected. Tumor tissue from each animal was snap frozen in liquid nitrogen and pulverized with a mortar and pestle.

KARPAS-422 cells were harvested during mid-log phase growth, and resuspended in Hank balanced salt solution with 50% Matrigel (BD Biosciences). Balb/C-nu mice (Charles River Laboratories Japan) received 1×10^7 cells (0.1 mL cell suspension) subcutaneously in the right flank. Mice carrying tumors of approximately 150 mm^3 for efficacy studies (14 days after injection) or 250 mm^3 for pharmacodynamics studies (21 days after injection) were sorted into treatment groups with similar mean tumor volumes. EPZ-6438 or vehicle (0.5% MC + 0.1% Tween-80 in water) was administered at the indicated doses on twice a day or once a day schedules for either 7 or 28 days by oral gavage. Each dose was delivered in a volume of 0.2 mL/20 g mouse (10 mL/kg), and adjusted for the last recorded weight of individual animals. Tumor volumes were followed throughout the experiment. Tumor volume was measured 2 times weekly after the start of treatment. In pharmacodynamic studies, tumors were harvested from specified mice, soaked in ice cold lysis buffer (10 mmol/L $MgCl_2$, 10 mmol/L Tris-HCl, 25 mmol/L KCl, 1% Triton X-100, 8.6% sucrose and protease inhibitor), and homogenized with handy microhomogenizer.

Pfeiffer donor tumors were first prepared by implanting 1×10^7 cells (0.1 mL cell suspension with 50% Matrigel; BD Biosciences) under the right arm of NSG mice (The Jackson Laboratory) subcutaneously. Approximately 63 days after implantation, donor tumors were harvested and dissected into fragments in size of approximate 20 mg. These tumor fragments were subsequently implanted into 100 NSG mice subcutaneously. Thirty days after implantation, 45 mice with tumors ranging from 124 to 680 mm^3 were selected and randomized into groups for efficacy study. EPZ-6438 or vehicle (0.5% MC + 0.1% Tween-80 in water) was administered at once a day schedules for either 7, 12, or 28 days by oral gavage. Each dose was delivered in a volume of 0.2 mL/20 g mouse (10 mL/kg), and adjusted for the last recorded weight of individual animals. Tumor volume was measured 2 times weekly after the start of treatment.

Rat studies

Male and female Sprague-Dawley rats (8 weeks old) were treated with EPZ-6438 at various doses or vehicle (0.5% NaCMC + 0.1% Tween-80 in water) for 28 days once a day. On day 22, the females from the highest dose group received another dose and were subsequently euthanized on day 23 approximately 29 hours after the last dose. All other animals were euthanized on day 29 approximately 29 hours after the last dose administered on day 28. At euthanasia, the full blood volume was collected, peripheral blood mononuclear cells (PBMC) were isolated, and cell pellets were frozen and stored at

−80°C before analysis. A 2-mm-thick slice of skin was formalin-fixed for 24 hours and transferred to 70% ethanol. The fixed tissues were paraffin embedded. Bone marrow samples were collected from femur, tibia, and hip bones, frozen and stored at −80°C before analysis. Histones extraction from tissues and H3K27Me3 ELISA were previously described (21).

Immunohistochemistry

Paraffin sections of skin were generated using a Leica rotary microtome RM2255 and placed on charged slides (SurgiPath). Slides were baked at 60°C for 30 minutes. Thereafter, slides were washed once with Bond Dewax solution (Leica Microsystems, Catalog No. AR9222), followed by 3 washes with absolute ethanol and then once with Leica Bond Wash solution (10× Bond wash, Leica Microsystems, Catalog No. AR9590, was used to prepare a 1× working solution in deionized water). Heat-mediated epitope retrieval was performed in Leica Bond ER2 retrieval solution (Leica Microsystems, Catalog No. AR9640), applied at ambient temperature 2 times followed by an incubation at 100°C for 20 minutes, and then at ambient temperature again for 12 minutes. After that slides were incubated with 3% H_2O_2 for 15 minutes, followed by 3 washes with Bond Wash solution. Antibody staining was done in a Leica Bond Max autostainer, Leica Microsystems M211518. Slides were incubated with primary antibody dilutions (anti-H3K27Me3, Cell Signaling Technology #9733; final concentration 0.07 μg/mL or anticleaved caspase-3, Epitomics #1476-1, final concentration 2 μg/mL) for 60 minutes, followed by 3 washes with Leica Bond Wash solution. Thereafter, slides were incubated with polymer horseradish peroxidase reagent (Leica Microsystems, Catalog No. DS9800) for 30 minutes followed by 4 washes with Leica Bond Wash solution and 1 wash with deionized water. Then slides were incubated with the DAB Refine chromogen for 10 minutes followed by 3 washes with deionized water. Slides were counterstained with hematoxylin for 5 minutes and washed once with deionized water and Leica Bond Wash. Dehydration and mounting of the stained slides were done in a Leica ST5020 autostainer and CV5030-TS5025 Coversliper (once 95% ethanol, 3 times 100% ethanol, and 3 times xylene). The mounting solution was Surgipath Micromount mounting medium (Leica Microsystems, Catalog No. 01730). Slides were digitized using the Aperio XT Scanner. Digitized slides were examined visually using Aperio Image Scope and image analysis, and quantification of the staining (percent of positive cells or percent positively stained area of the sample) was done using the Aperio image algorithms.

Results

EPZ-6438 specifically inhibits cellular H3K27 methylation in cells

A preliminary description of EPZ-6438 was reported previously (21). EPZ-6438 (structure shown in Fig. 1A) is a potent, selective, and orally bioavailable small molecule inhibitor of EZH2 showing context-specific activity in *SMARCB1*-deleted rhabdoid tumors. Similar to its effect in rhabdoid tumor cells, EPZ-6438 treatment of the *EZH2*

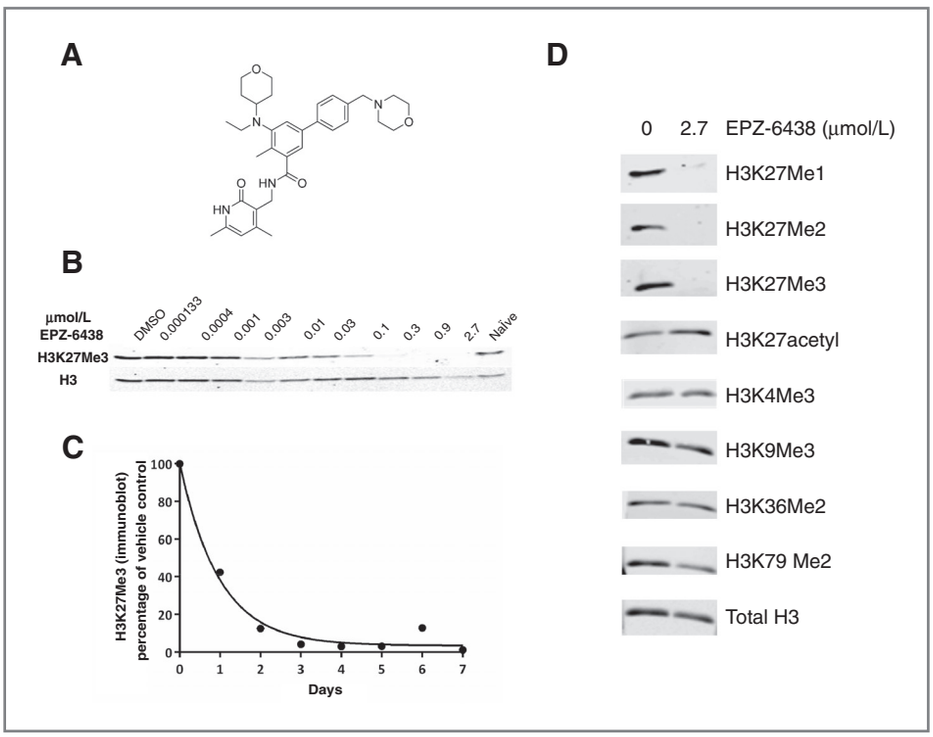

Figure 1. Effects of EPZ-6438 on cellular global histone methylation and cell viability. A, chemical structure of EPZ-6438. B, concentration-dependent inhibition of cellular H3K27Me3 levels in *EZH2* Y646 mutant–bearing WSU-DLCL2 cells, determined by immunoblot. C, EPZ-6438 inhibits cellular H3K27Me3 in WSU-DLCL2 cells in a time-dependent manner (assessed by immunoblot and densitometry). D, EPZ-6438 selectively inhibits cellular H3K27 methylation in OCI-LY-19 *EZH2* wild-type lymphoma cells. Cells were treated for 4 days for each experiment shown at the indicated concentrations (1 μmol/L in B).

Table 1. IC_{50} values for methylation and proliferation as well as LCC values for EPZ-6438 in human lymphoma cell lines

Cell line	*EZH2* status	Methylation IC_{50} (nmol/L)[a]	Proliferation IC_{50} (μmol/L)[b]	LCC (μmol/L)[b]
DOHH-2	Wild-type	3	1.7	>10
Farage	Wild-type	2	0.099	>10
OCI-LY19	Wild-type	8	6.2	>10
Toledo	Wild-type	ND	7.6	>10
KARPAS-422	Y646N	90	0.0018	0.12
Pfeiffer	A682G	2	0.00049	0.0005
RL	Y646N	22	5.8	>10
SU-DHL-10	Y646F	ND	0.0058	0.14
SU-DHL-6	Y646N	20	0.0047	0.21
WSU-DLCL2	Y646F	9	0.0086	0.17

Abbreviation: ND, not determined.

[a]Derived after incubation for 4 days by immunoblot. Values represent the result from 1 experiment.

[b]Derived after incubation for 11 days. Compound incubations for each experiment were performed in triplicate, and values represent 1 experiment for all cell lines except OCI-LY19, Pfeiffer, and WSU-DLCL2. For the remaining 3 cell lines, values represent the mean from the following number of experiments: OCI-LY19, $n = 9$; Pfeiffer, $n = 2$; and WSU-DLCL2, $n = 15$.

Y646F-mutant lymphoma cell line WSU-DLCL2 for 4 days induced a concentration-dependent reduction in global H3K27Me3 levels with an IC_{50} value of 9 nmol/L (H3K27Me3 levels determined by immunoblot; Fig. 1B and Table 1). Treatment of WSU-DLCL2 cells with 1 μmol/L EPZ-6438 led to time-dependent global loss of H3K27Me3 with a half-life of approximately 1 day. Consistent with a simple exponential decay process, we observed ≥90% loss of H3K27Me3 after 3 to 4 days of compound treatment (Fig. 1C). To test the specificity of EPZ-6438 in cells, we chose an *EZH2* wild-type line because mutant cells, including WSU-DLCL2, do not contain detectable levels of the dimethyl form of H3K27 (14). When we incubated OCI-LY19 *EZH2* wild-type lymphoma cells with 2.7 μmol/L EPZ-6438 for 4 days, the only methyl marks affected were H3K27Me1, H3K27Me2, and H3K27Me3, the 3 known products of PRC2 catalysis (Fig. 1D). Incubation with EPZ-6438 also resulted in a slight increase in H3K27 acetylation. Furthermore, lysine 36 dimethylation of histone H3 was not influenced.

The ability of EPZ-6438 to reduce global H3K27Me3 levels was further tested in several other human lymphoma cell lines, including lines expressing either wild-type or mutant EZH2. EPZ-6438 reduced H3K27Me3 with similar potency in all cell lines, independent of the *EZH2* status (Table 1).

EPZ-6438 leads to selective killing of lymphoma cell lines bearing EZH2 point mutations

To evaluate the phenotypic effects of compound treatment, we performed proliferation assays with wild-type and mutant lymphoma cell lines. Incubation of WSU-DLCL2 *EZH2* Y646F-mutant cells with EPZ-6438 inhibited cell proliferation with an average IC_{50} value of 0.28 ± 0.14 μmol/L in a 6-day proliferation assay. To evaluate the kinetics of the antiproliferative activity of EPZ-6438 in more detail, additional proliferation assays were performed over a period of 11 days. In WSU-DLCL2 cells, the antiproliferative effect of EPZ-6438 was apparent after 4 days of incubation (Fig. 2A). This coincides with the time required for maximal H3K27Me3 inhibition in this cell line (Fig. 1B) and is consistent with a mechanism in which phenotypic effects occur following inhibition of H3K27 methylation. The IC_{50} value for EPZ-6438 inhibition of proliferation of WSU-DLCL2 cells was lower after 11 days of treatment than after 6 days of treatment (Table 1), likely because of increase cell killing at later time points. In contrast to the WSU-DLCL2 cells, the proliferation of OCI-LY19 human lymphoma cells (*EZH2* wild-type for residue Y646) over 11 days was not significantly affected (Fig. 2B), despite comparable IC_{50} values for H3K27Me3 inhibition in both cell lines (Table 1). The 11-day proliferation assay results were used to calculate the lowest cytotoxic concentration (LCC), for each cell line. The LCC is defined as the concentration of inhibitor at which the proliferation rate becomes zero and represents the crossover point between cytostasis and cytotoxicity (17). The LCC value for WSU-DLCL2 *EZH2* Y646F-mutant human lymphoma cells was 0.17 μmol/L whereas no cytotoxicity (LCC > 10 μmol/L) was observed in the *EZH2* wild-type cell line OCI-LY19 (Table 1). This context-specific activity of EPZ-6438 was further supported by results from 11-day proliferation assays with an extended lymphoma cell line panel. All cell lines harboring an *EZH2* mutation, with the exception of the RL cell line (*EZH2* Y646N), were more sensitive to the antiproliferative effects of EPZ-6438 than cell lines containing wild-type *EZH2* (Table 1). Farage cells had the lowest IC_{50} among the *EZH2* wild-type group, but no cytotoxicity could be observed with compound treatment (LCC > 10 μmol/L).

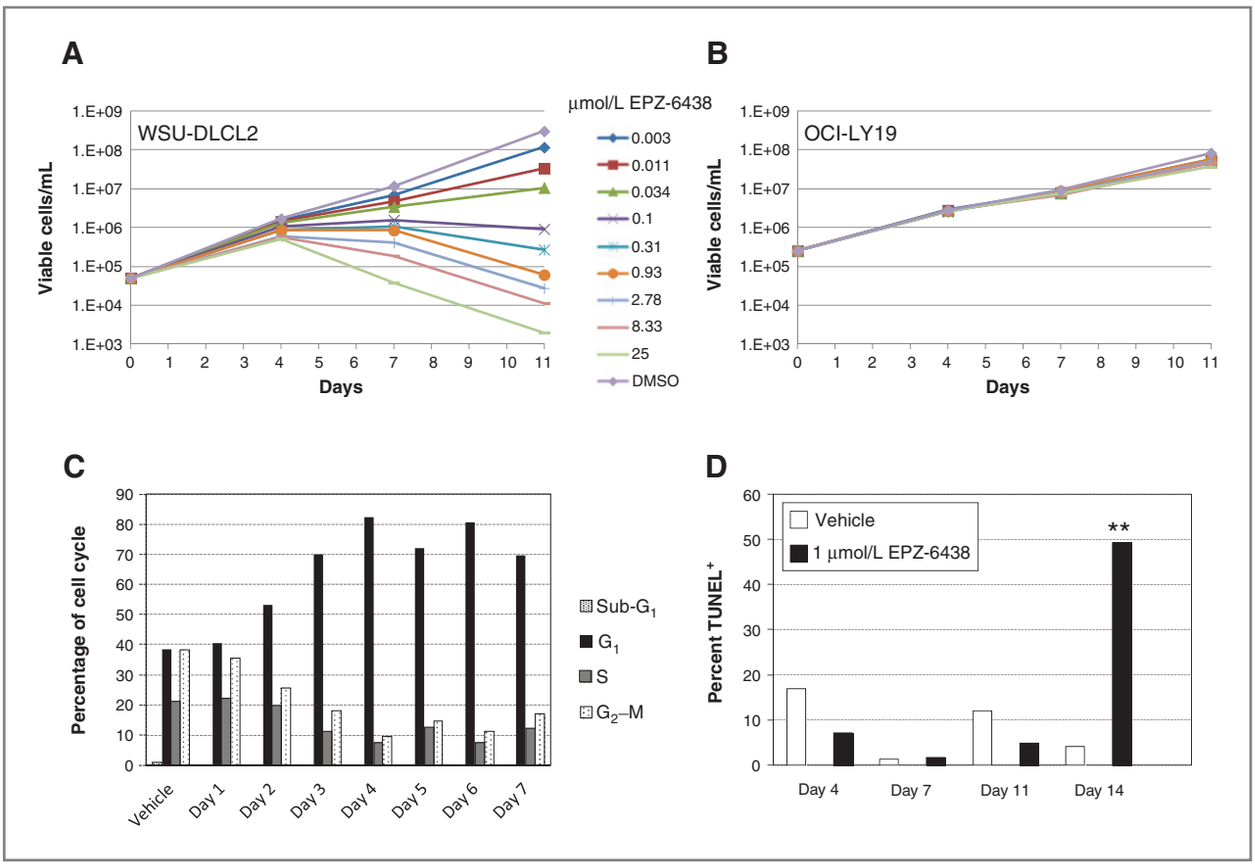

Figure 2. EPZ-6438 specifically inhibits the proliferation of *EZH2*-mutant lymphoma cells *in vitro* through cell-cycle arrest and induction of apoptosis. A and B, selective inhibition of proliferation of *EZH2*-mutant cells by EPZ-6438 *in vitro* (measured by flow cytometry). WSU-DLCL2 *EZH2* Y646F-mutant (A) and OCI-LY19 *EZH2* wild-type cells (B) were replated at the original seeding densities on days 4 and 7. Each point represents the mean for each concentration ($n = 3$). C, cell-cycle analysis (by flow cytometry) in WSU-DLCL2 cells during incubation with either vehicle or 1 μmol/L EPZ-6438 for up to 7 days. Cells were split and replated on day 4 at the original seeding density. G_1 arrest is observed. D, determination of apoptosis (by TUNEL assay) in WSU-DLCL2 cells during incubation with either vehicle or 1 μmol/L EPZ-6438 for up to 14 days. Cells were split and replated on days 4, 7, and 11 at the original seeding density. Apoptosis was induced on day 14. **, $P < 0.01$, Student *t* test.

The Pfeiffer cell line (*EZH2* A682G) showed a 20- to 300-fold increase in sensitivity to EPZ-6438, as measured by IC_{50} value and LCC, respectively, over the Y646-mutant cell lines.

We also investigated the minimum time of compound exposure necessary for sustained cell killing by washout experiments. The LCC values on day 14 for WSU-DLCL2 cells that were either incubated with EPZ-6438 for 7 days (followed by 7 days of compound washout) or continuously for 14 days were similar (Supplementary Table S1). Drug exposure for only 4 days with 10-day washout also induced cytotoxic effects albeit with lower potency (higher LCC value).

EPZ-6438 induces G_1 arrest and apoptosis in EZH2-mutant lymphoma cells

We assessed the effects of incubation with EPZ-6438 (1 μmol/L) for 7 days on cell-cycle progression and apoptosis in WSU-DLCL2 cells. A time-dependent increase in the percentage of cells in G_1 phase, and a decrease in the percentage of cells in S phase and G_2–M phase was apparent with EPZ-6438 incubation with a half-life of approximately 2 days (Figs. 2C and Supplementary Fig. S1D); the maximum effect was achieved after 4 days. There was no apparent increase in the sub-G_1 fraction, suggesting that apoptosis was not induced by EPZ-6438 incubation for 7 days. This is in agreement with the growth curves of WSU-DLCL2 cells in the presence of EPZ-6438, which show that more than 7 days of incubation are required for robust cytotoxic effects (Fig. 2A). Analysis of apoptosis by terminal deoxynucleotidyl transferase–mediated dUTP nick end labeling (TUNEL) assay in an extended incubation of WSU-DLCL2 cells with EPZ-6438 revealed that EPZ-6438–mediated cell death occurred through the induction of apoptosis sometime between day 11 and day 14 (Fig. 2D).

To gain additional insights into the mechanism of the antiproliferative effects of EPZ-6438, we performed a gene expression profiling experiment with 4 different *EZH2* mutant–bearing lymphoma cells (WSU-DLCL2, SU-DHL-

6, Pfeiffer, and KARPAS-422) treated with compound for 2, 4, and 6 days at concentrations equivalent to LCC or 10× LCC for each cell line. The mRNA levels of PRC2 complex members were not significantly changed with treatment (e.g., WSU-DLCL2 at 10× LCC; Supplementary Fig. S2A). Because PRC2 mainly functions as a transcriptional repressor, upregulation of the target genes was expected. Our results confirmed that a subset of genes previously identified as PRC2/EZH2 targets in ES cells (22) or germinal center B cells (23) were upregulated in one or more of the *EZH2*-mutant cell lines upon EPZ-6438 treatment (Supplementary Fig. S2B–S2D). In addition, downregulation of genes in some cell lines was also observed, particularly at later time points (Supplementary Fig. S2E); a finding consistent with studies reported in the literature using EI1, another EZH2 inhibitor (20).

To assess the effects of EPZ-6438 on H3K27Me3 at individual gene loci, we performed ChIP-PCR at 5 known PRC2 target gene promoters (23) and observed a range of H3K27Me3 diminution (Supplementary Fig. S1A). Consistent with alleviation of the repressive H3K27Me3 mark, these 5 target genes were also shown to increase in expression upon treatment with EPZ-6438 (Supplementary Fig. S1A). In addition, we evaluated the effects of EPZ-6438 on PRC2 complex promoter occupancy by performing ChIP-PCR on both EZH2 and SUZ12 (Supplementary Fig. S1B and S2C). At 3 of the 5 gene promoters PRC2 member occupancy was reduced, but not eliminated. PRC2 occupancy actually increased at the remaining 2 promoters. Interestingly, for those promoters with increased PCR2 member occupancy after compound treatment, H3K27Me3 reduction was more limited. In all cases tested, the change in EZH2 versus SUZ12 promoter occupancy was similar in direction and magnitude, consistent with the data that EPZ-6438 inhibits EZH2 by a SAM-competitive mechanism, rather than by disrupting the PRC2 complex.

Interestingly, very few gene changes were observed in the Pfeiffer cell line, compared with the 3 *EZH2* Y646-mutant cell lines despite our use of an EPZ-6438 concentration that gave profound phenotypic effects. The relatively limited gene expression changes observed in Pfeiffer cells meant that a post dose gene expression signature common to all 4 cell lines could not be derived. Even when we considered the *EZH2* Y646-mutant cell lines alone, only 13 genes were commonly upregulated (Supplementary Table S2A, group A). This is similar to the findings of McCabe and colleagues using GSK126 (another EZH2 inhibitor), where only 35 genes overlapped in 4 of 5 cell lines profiled (19). The most altered (up- or downregulated) genes in each cell line or genes commonly altered in pairs of cell lines are presented Supplementary Table S2A. In addition to analyzing mRNA levels of specific genes, we also performed pathway and gene set level analysis to gain mechanistic insight. Ingenuity Pathway Analyses on the sets of differentially expressed genes upon EPZ-6438 treatment pointed to many pathways being significantly enriched in each cell line with the exception of Pfeiffer; however, they were not common among all cell lines. When we performed gene set enrichment analysis of the data, we found that gene sets of the cell cycle and spliceosome pathways, as well as groups of genes containing E2F-binding motifs, were negatively enriched (i.e., downregulated with treatment) among all cell lines, including Pfeiffer (Supplementary Tables S2B–S2D). This was observed after only 2 days of compound treatment in some cell lines, which is consistent with the timing of cell cycle changes after compound addition (Fig. 2C). Similar changes were also observed with our previously published EZH2 inhibitor tool compound EPZ005687 (17). Genes that were commonly altered in all cell lines that correlated with the cell-cycle effects mediated by EPZ-6438 are shown in Supplementary Fig. S1E.

Oral administration of EPZ-6438 leads to target inhibition in EZH2-mutant xenograft models in mice

The pharmacokinetic properties of EPZ-6438 were characterized in both mouse and rat following intravenous and oral administration. EPZ-6438 showed low clearance in mouse with a steady-state volume of distribution (VDss) 1.5-fold higher than total body water, whereas in rat, clearance was moderate with a VDss 3.3-fold higher than total body water (Supplementary Fig. S3). Following oral administration in both species, EPZ-6438 was rapidly absorbed with maximal concentrations achieved in 15 to 18 minutes after dose. In addition, the mean residence time was 2 hours in both species with an elimination $t_{1/2}$ of 4 and 5 hours in mouse and rat, respectively. The oral bioavailability of a suspension formulation was 15% in rat and 55% in mouse. We next evaluated whether oral dosing of EPZ-6438 leads to *in vivo* target inhibition in mice bearing *EZH2*-mutant lymphoma xenografts. SCID mice implanted subcutaneously with WSU-DLCL2 xenografts were orally dosed with EPZ-6438 for 7 days. Determination of EPZ-6438 plasma levels 5 minutes before and 3 hours after the last dose revealed a clear dose-dependent exposure (Supplementary Fig. S4A). Only animals dosed at 160 mg/kg 3 times a day or 213 mg/kg twice a day maintained mean compound plasma levels above the WSU-DLCL2 cell LCC (1,652 ng/mL, adjusted for mouse plasma protein binding) throughout the dosing cycle. EPZ-6438 concentrations in plasma and in tumor homogenates measured 3 hours after the last dose were comparable, especially in the highest dose groups (Supplementary Fig. S4B). This indicates that EPZ-6438 distributes effectively into tumor tissue. When we analyzed H3K27Me3 levels in tumors, dose-dependent EZH2 target inhibition was observed (Fig. 3A and B). H3K27Me3 inhibition was less in tumors from mice dosed at 213 mg/kg once a day compared with 160 mg/kg 3 times a day or 213 mg/kg twice a day, suggesting that maintaining a plasma concentration above LCC throughout a dosing cycle is optimal for maximum target inhibition. We performed a similar 7-day study in nude mice implanted subcutaneously with KARPAS-422 xenografts

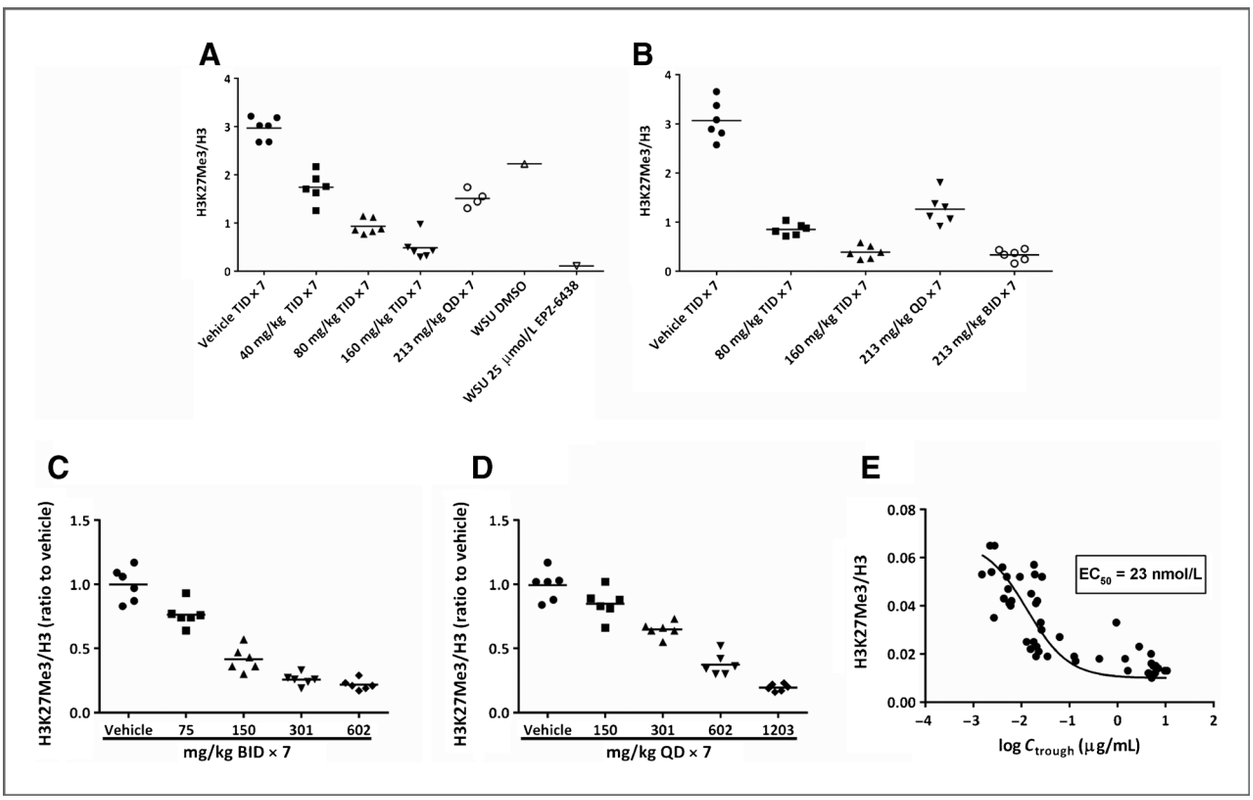

Figure 3. Target inhibition in lymphoma xenograft tumors from mice treated with EPZ-6438 for 7 days, measured by ELISA. A and B, each point shows the ratio of H3K27Me3 to total H3 of histones extracted from WSU-DLCL2 xenograft tumors from SCID mice dosed as indicated. Tumors were harvested 3 hours after the last dose on day 7. Horizontal lines represent group mean values. Two independent ELISAs were performed containing comparisons for different groups. Histones extracted from WSU-DLCL2 cells incubated with 25 μmol/L EPZ-6438 or DMSO for 4 days *in vitro* were included as controls. C and D, each point shows the ratio of H3K27Me3 to total H3, normalized to the mean of the respective vehicle control, of histones extracted from KARPAS-422 xenograft tumors from balb/c-nu mice dosed as indicated. Tumors were harvested 3 hours after the last dose on day 7. Horizontal lines represent group mean values. E, during the KAPRAS-422 study (C and D) plasma drug concentrations were determined before the last dose on day 7 (C_{trough}) and plotted against individual tumor H3K27Me3 levels to calculate the EC_{50} value for methylation inhibition *in vivo*. BID, twice a day; QD, once a day; TID, 3 times a day.

assessing both twice a day and once a day dosing schedules. EPZ-6438 induced a dose-dependent reduction of tumor H3K27Me3 levels with both regimens with an EC_{50} value of 23 nmol/L (Fig. 3C–E).

EPZ-6438 induces significant antitumor effects, including complete and sustained regressions, in multiple EZH2-mutant lymphoma xenografts

We next performed a series of 28-day lymphoma xenograft efficacy studies in mice to assess *in vivo* antitumor activity of EPZ-6438. EPZ-6438 induced dose-dependent tumor growth inhibition (TGI) in SCID mice bearing WSU-DLCL2 *EZH2* Y646F-mutant xenograft tumors. The highest dose of 160 mg/kg 3 times a day gave the maximum TGI of 58% in this model (Fig. 4A). This was also the only dose group in which animals maintained mean EPZ-6438 plasma levels above LCC for WSU-DLCL2 cells throughout the dosing cycle (Supplementary Fig. S4C). EPZ-6438 levels in tumor tissue homogenates were also determined (Supplementary Fig. S4D). ELISA analysis of H3K27Me3 levels in histones from tumors collected on day 28 indicated dose-dependent target inhibition with maximal inhibition achieved at 150 mg/kg 3 times a day (Supplementary Fig. S5A). H3K27Me3 levels in WSU-DLCL2 xenografts were lower in mice dosed for 28 days compared with 7 days indicating that prolonged administration of EPZ-6438 increased the degree of target inhibition. More dramatic antitumor activity was seen when EPZ-6438 was tested in a KARPAS-422 *EZH2* Y646N-mutant xenograft model. EPZ-6438 was administered more than a 28-day period on a twice a day schedule. TGI of 87% was observed at the lowest dose of 80.5 mg/kg twice a day (Fig. 4B). Strikingly, both of the higher doses (161 and 322 mg/kg twice a day) completely eradicated the xenograft tumors. A second KARPAS-422 xenograft study was performed in which EPZ-6438 was dosed at 322 and 644 mg/kg twice a day for 28 days followed by an extended observation period (Supplementary Fig. S5B and S5C). As in the first study, tumors were completely eradicated at both doses by day 28. Furthermore, no tumor regrowth was observed for up to 63 days after cessation of dosing until the study was terminated on day 92. We also

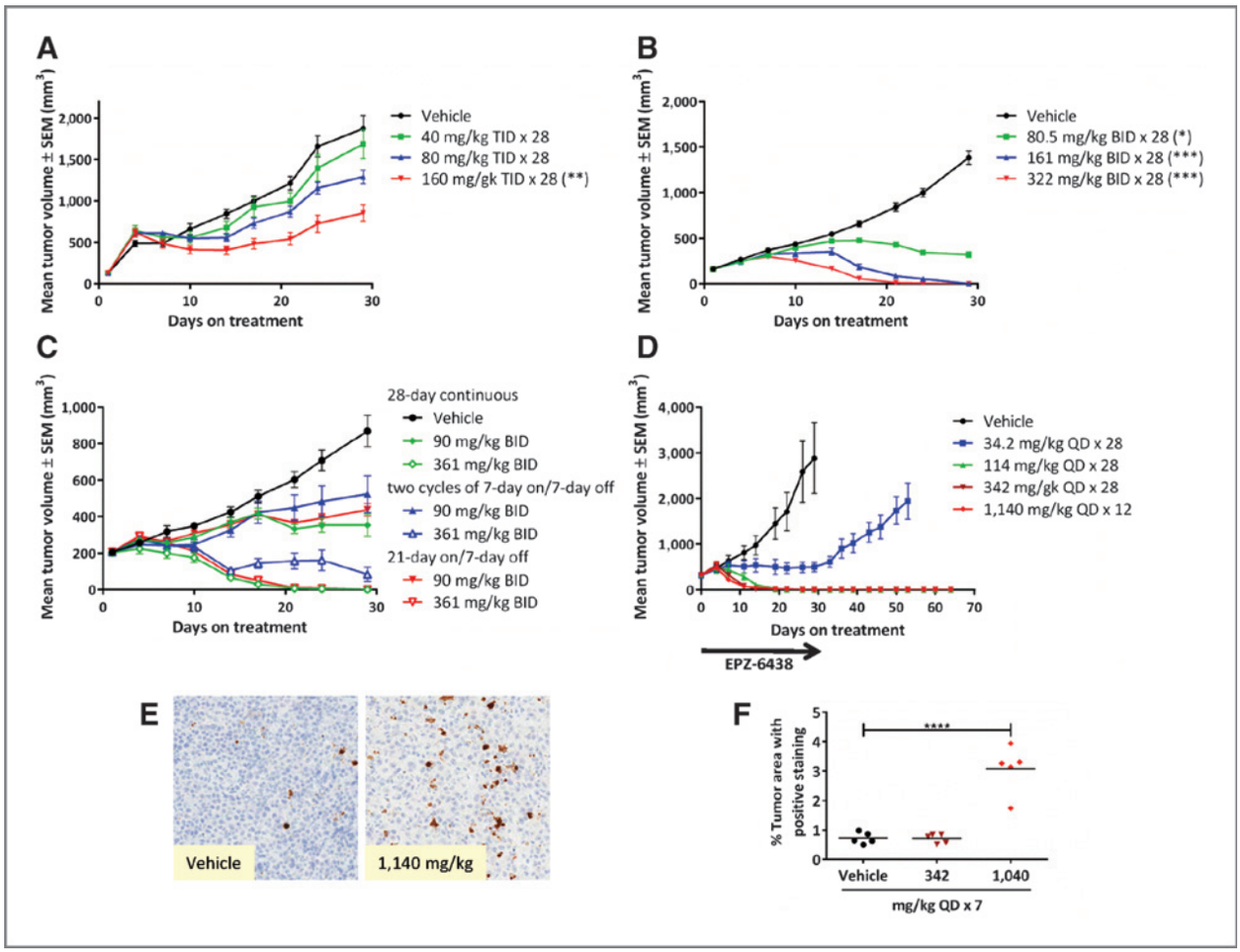

Figure 4. EPZ-6438 demonstrates strong antitumor activity in several *EZH2*-mutant lymphoma xenograft models. A, WSU-DLCL2 lymphoma xenograft tumor growth inhibition with 3 times a day (TID) dosing of EPZ-6438 for 28 days. Data, mean ± SEM ($n = 12$). B, tumor regressions of KARPAS-422 lymphoma xenografts in mice dosed with EPZ-6438 twice a day (BID) for 28 days. Data, mean ± SEM ($n = 9$). C, tumor growth inhibition and regressions of KARPAS-422 xenografts in mice dosed with 3 different dosing schedules of EPZ-6438. Data, mean ± SEM ($n = 8$ for the 361 mg/kg in 2 cycles of 7-day on/7-day off group; $n = 9$ for all other groups). D, tumor regressions induced by once a day (QD) dosing of EPZ-6438 of mice bearing Pfeiffer lymphoma xenografts. Data, mean tumor volumes ± SEM ($n = 9$). For all animals, once a day dosing was performed from day 1 to day 28, except for mice administered 1,140 mg/kg (dosing ended on day 12). Tumor growth in mice was followed after dosing stop for another 36 days, and no regrowth was observed at 3 of 4 dose levels. *, $P < 0.05$; **, $P < 0.01$; ***, $P < 0.001$; repeated measures ANOVA, Dunnett posttest. E and F, tumor tissue from Pfeiffer xenograft-bearing mice was collected after 7 days of EPZ-6438 administration at the indicated doses and subjected to immunohistochemical analysis for cleaved caspase-3 (indicating apoptosis). Positive cells were quantified by image analysis. ****, $P < 0.0001$; Dunnett multiple comparison test.

investigated intermittent dosing schedules in KARPAS-422 xenograft-bearing mice. EPZ-6438 showed significant dose-dependent antitumor effects with 2 cycles of 7-day on/7-day off and 21-day on/7-day off schedules (Fig. 4C). For all dosing schedules, tumor growth inhibition and complete regressions were observed at 90 and 361 mg/kg twice a day, respectively. The Pfeiffer *EZH2* A682G-mutant xenograft model was the most sensitive tumor model, as suggested by the potent antiproliferative effects of EPZ-6438 on this cell line *in vitro*. All EPZ-6438 dose groups (once a day schedule) except the lowest one (34.2 mg/kg once a day) showed complete tumor regressions in all animals (Fig. 4D). Again, tumor regrowth was not observed up to the end of the study (36 days after stopping EPZ-6438 administration). The low dose of 34.2 mg/kg once a day induced tumor stasis rather than complete regressions during the administration period and tumor regrowth occurred following cessation of dosing. Pfeiffer xenograft-bearing mice from a parallel cohort were treated only for 7 days at the same doses, and tumors were analyzed for induction of apoptosis by immunohistochemistry for cleaved caspase-3. A clear increase of cleaved caspase-3 positive cells was observed on day 7 for the highest dose group (Fig. 4E and F). EPZ-6438 was well tolerated with minimal effect on body weight at all doses below 1,140 mg/kg once a day (Supplementary

Fig. S6). Because of body weight loss dosing was stopped on day 12 for mice administered 1,140 mg/kg once a day; nevertheless, complete and durable regressions were observed in this group, despite being exposed to EPZ-6438 for only 12 days.

EPZ-6438 inhibits H3K27 methylation in nontumor tissues in a dose-dependent manner

The profound and sustained regressions in the preclinical models described above suggest that EPZ-6438 may represent an exciting new treatment modality for subsets of NHL. Measuring pharmacodynamic biomarker modulation postdose is often performed in early clinical trials to assess the degree of target inhibition/engagement required to produce a clinical or biologic response, based on data from preclinical models. Because the collection of postdose tumor biopsies is often not possible, easily accessible surrogate tissues, such as PBMCs, skin or bone marrow are often collected instead. To test EZH2 target inhibition in surrogate tissues, male and female Sprague Dawley rats were orally administered 100, 300, or 1,000 mg/kg EPZ-6438 once a day for 28 days, and PBMCs, bone marrow, and skin samples were collected at study end. Because of body weight loss, females in the 1,000 mg/kg group had to be euthanized on day 23. Dose-dependent target inhibition was observed in PBMCs and bone marrow from rats dosed with EPZ-6438, as measured by ELISA (Fig. 5A and B). The degree of target inhibition was less pronounced for PBMCs from females that were dosed for 22 days compared with males that were dosed for 28 days (same dose of 1,000 mg/kg). A dose-dependent reduction in H3K27Me3 positive cells was observed in the epidermis of skin of EPZ-6438-dosed rats, as assessed by an immunohistochemistry assay (Fig. 5C). The maximum effect was observed at the highest dose, and was already evident after 22 days of EPZ-6438 administration. Compound exposure was higher in female rats compared with males (Fig. 5D), which may explain the higher degree of target inhibition in females, especially at 100 and 300 mg/kg.

Discussion

The critical role of genetic alterations for oncogenesis has been well established through a combination of DNA molecular analysis of primary tumor tissue (e.g., sequencing and copy number analysis) and correlated functional studies in preclinical models (24, 25). Recently, there has been a growing appreciation for the impact of changes of the epigenome—of paramount importance in regulation of gene expression—as a similarly important hallmark of cancer (26, 27).

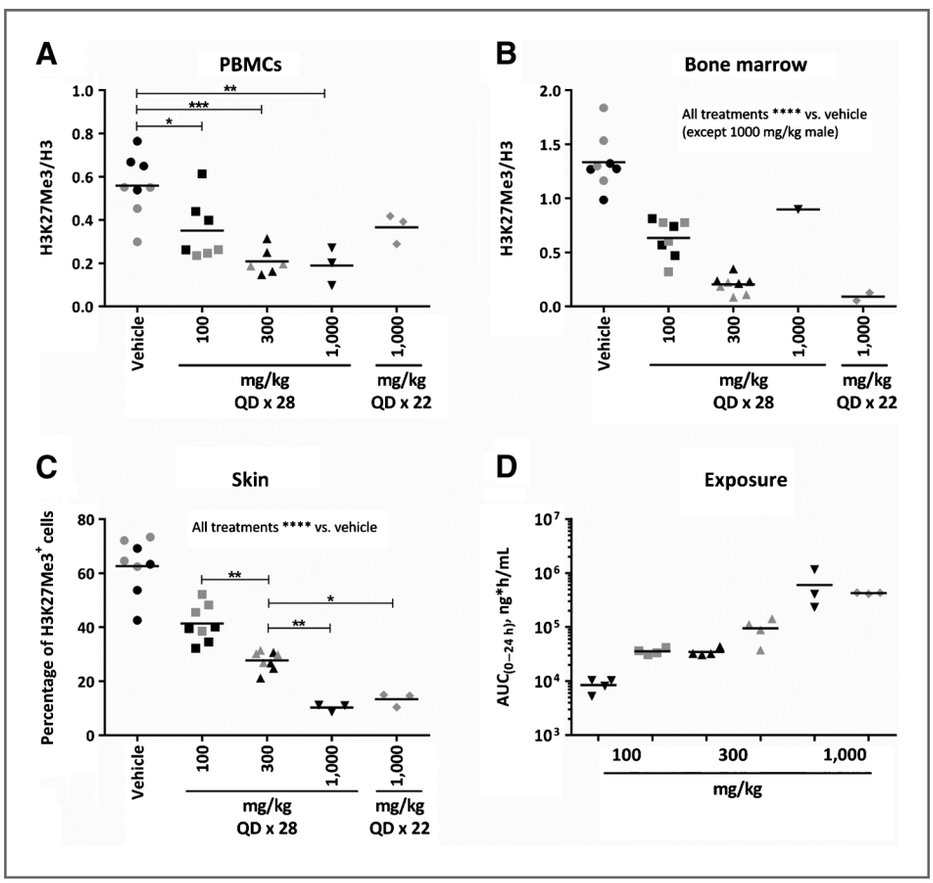

Figure 5. EZH2 target inhibition in normal tissues from rats administered with EPZ-6438 for 22 or 28 days. Inhibition of H3K27Me3 levels in rat peripheral blood mononuclear cells (A) and rat bone marrow (B) after administration of EPZ-6438, measured by ELISA. Individual symbols represent the ratio of H3K27Me3 to total H3 for histones extracted from individual tissues; horizontal lines represent mean values. C, target inhibition in rat skin (epidermal compartment) after dosing with EPZ-6438, measured by immunohistochemistry. Individual symbols represent the percentage of H3K27Me3-positive cells for tissue from individual animals; horizontal lines represent mean values. D, exposures on day 28 or day 22 (1,000 mg/kg females). Individual symbols represent AUC values for individual animals; horizontal lines represent mean values. Black symbols are males, gray symbols are females. *, $P < 0.05$; **, $P < 0.01$; ***, $P < 0.001$; ****, $P < 0.0001$, one-way ANOVA, Bonferroni posttest. QD, once a day.

Epigenetic regulation of gene expression is based on spatial and temporal orchestration of a spectrum of covalent modifications to chromatin. Of particular importance in regulating the fidelity of gene expression is site-specific histone protein methylation at lysine and arginine amino acids, a group of reactions catalyzed by the protein methyltransferase (PMT) class of group-transfer enzymes (28). A number of PMTs have been shown to be altered in genetically defined human cancers, and these alterations have further been shown to be drivers of the specific cancers (i.e., the alterations are oncogenic; ref. 3).

The PRC2 enzyme complex is the only PMT in humans known to catalyze the site-specific methylation of the H3K27 site (4, 5). Several members of the PRC2 complex, including the catalytic subunit EZH2, have been reported to be altered in a spectrum of human tumors (6). As described earlier, a cluster of point mutations within the catalytic SET domain of EZH2 have been found in approximately 10% of patients with NHL, and these have been shown to alter substrate utilization in such a way as to drive a hyper-trimethylated H3K27 phenotype in the mutant-bearing cells that is suggested to aid in lymphomagenesis (8, 14). We and others have reported selective tool compound inhibitors of wild-type and mutant EZH2 as chemical probes with which to demonstrate the dependence of *EZH2*-mutant NHL cell lines on PRC2 activity in cell culture and *in vivo* (17–20). These various tool compounds, however, lacked suitable pharmacologic properties for advancement into human clinical trials.

EPZ-6438 is a pharmacologically improved EZH2 inhibitor with *in vitro* properties similar to our previously reported tool compound EPZ005687 (17), but with superior potency and oral bioavailability (Supplementary Fig. S3). A brief description of EPZ-6438 was provided in a recent report where we demonstrated the utility of this compound in treating malignant rhabdoid tumors deficient in the SWI/SNF complex component SMARCB1 (also referred to as INI1 or hSNF5; ref. 21). In this report, we have demonstrated that treatment with EPZ-6438 leads to a global and specific inhibition of PRC2 substrate methylation (H3K27) in a range of NHL cells. Cytotoxic, antiproliferative effects were specifically observed in NHL cells bearing *EZH2* mutations, and gene expression profiling studies confirmed that EPZ-6438 treatment led to de-repression of known PRC2 target genes. ChIP-PCR of the promoters of 5 known PRC2 targets revealed that their de-repression correlated with overall decreased promoter H3K27Me3 levels. The effect of EPZ-6438 treatment on PRC2 complex occupancy varied across the genes analyzed and included increases, decreases, and no changes in occupancy. However, for any given gene promoter analyzed, the effect of EPZ-6438 treatment on individual PRC2 complex members was similar (in direction and magnitude). This observation is consistent with the enzymatic data demonstrating that EPZ-6438 inhibits EZH2 through a SAM-competitive mechanism and is counter to the notion that this inhibitor disrupts the formation of the PRC2 complex itself. Notably, at those promoters where H3K27Me3 inhibition is partial, PRC2 occupancy is increased with treatment. One could speculate that at such promoters, catalytic inhibition of EZH2 induces compensatory recruitment of more PRC2 complexes, delaying demethylation.

Although de-repression of known EZH2 target genes occurred in the cell lines tested, there was little overlap between gene expression signatures between different mutant lymphoma cell lines as reported in a previous study (19). Possible explanations could be cell line epigenetic diversification *in vitro* or inappropriate dynamic ranges of the gene expression assays used to detect small expression changes, as previously discussed (29). Our observation of very modest effects on gene expression in Pfeiffer cells contrasts with the results of McCabe and colleagues using GSK126 (another EZH2 inhibitor; ref. 19), in which robust gene expression changes were observed in the same cell line. This discrepancy may be because of their use of an inhibitor concentration equivalent to 50× the cellular H3K27Me3 IC_{50} compared with the use in this study of a much lower inhibitor concentration equivalent to 2.5× the cellular H3K27Me3 IC_{50}. Nevertheless, the fact that this concentration is 10× the Pfeiffer LCC suggests that a relatively small gene expression changes in Pfeiffer cells can trigger a robust antiproliferative response in this highly EZH2 pathway addicted cell line. EPZ-6438 treatment also caused downregulation of genes involved in cell-cycle and spliceosome pathways, as well as groups of genes containing E2F-binding motives. These gene expression changes could be indirect effects downstream of the relief of PRC2 inhibition, but may also be a direct effect of inhibiting an EZH2-activating function independent of the PRC2 complex, as recently suggested by others for STAT3 signaling in glioblastoma and androgen receptor signaling in prostate cancer (30, 31). This will be the focus of future studies. In addition, it has been reported that EZH2 is regulated by E2F itself in metastatic prostate cancer and in lymphomas, suggesting the existence of feed-forward loops (32).

Dosing of *EZH2*-mutant NHL xenograft-bearing mice with EPZ-6438 led to significant antitumor effects ranging from marked and dose-dependent tumor growth inhibition (e.g., WSU-DLCL2 xenografts) to complete and durable eradication of tumors (e.g., KARPAS-422 and Pfeiffer xenografts; Fig. 4). The *EZH2* A682G mutant–bearing Pfeiffer cell line was particularly sensitive to EZH2 inhibition, both *in vitro* and *in vivo*; relatively limited doses or short time dosing of EPZ-6438 resulted in complete and permanent elimination of Pfeiffer cell tumors in the mouse xenograft model. These preclinical data suggest that potent and selective EZH2 inhibitors, such as EPZ-6438, may be ideal candidates for development as a novel targeted therapy for treatment of patients with NHL with cancers bearing A682G-mutated EZH2.

The apparent differences in the *in vivo* response of WSU-DLCL2 and KARPAS-422 tumors was not predicted by the similar sensitivity of these 2 cell lines to EPZ-6438 treatment in cell culture (i.e., the 2 lines displayed similar

LCC values, as summarized in Table 1). This may suggest that in the *in vivo* context of the xenograft models, WSU-DLCL2 can utilize alternative pathways for cell growth and survival that partially circumvent the impact of EZH2 inhibition. Similarly, the reasons for the insensitivity of the *EZH2* Y646N-mutant lymphoma cell line RL *in vitro* are not understood at present, and may suggest the presence of parallel escape routes from inhibition of the EZH2 pathway. The insensitivity of RL cells to pharmacologic EZH2 inhibition was also observed by McCabe and colleagues with GSK126 (19). These observations require more in-depth study to determine the molecular origins of the differential effects of EZH2 inhibition on these cells. Interestingly, we also failed to induce significant resistance to EPZ-6438 by treating several inhibitor sensitive cell lines for >7 months *in vitro*.

Beguelin and colleagues recently suggested that germinal center derived DLBCLs are addicted to EZH2 independent of its mutational state, as impaired enzyme activity, for instance induced by EZH2 inhibitor treatment, showed antiproliferative activity in both *EZH2* wild-type and mutant cell lines (11). Our data suggest that EZH2 inhibition may affect *EZH2* wild-type GCB DLBCL cells by slowing their growth in a limited fashion (with micromolar IC_{50} values, except the Farage cell line); however, only the mutant cell lines are driven into cell death during the 11-day compound incubation period. This suggests EZH2 oncogene addiction and a superior potential for antitumor activity of EZH2 inhibitors in patients with *EZH2*-mutated GCB lymphoma compared with wild-type cases.

Taken together, the preclinical data presented here support the further development of EPZ-6438 as a new treatment modality for genetically defined subsets of NHL. This compound is currently under study as E7438 in a phase I trial of relapsed and refractory malignancies that have failed all standard therapy. The primary goal of the phase I trial is to establish the safety and define the maximal tolerated dose of the drug. The ability to measure dose-dependent changes in H3K27Me3 levels in skin, PBMCs, and bone marrow may also portend the use of signal from these surrogate tissues as a noninvasive pharmacodynamics biomarker during human clinical trials.

Disclosure of Potential Conflicts of Interest

S.K. Knutson, C.R. Klaus, A. Raimondi, N.J. Waters, R. Chesworth, R.A. Copeland, V.M. Richon, K.W. Kuntz, and H. Keilhack have ownership interest (including patents) in Epizyme. No potential conflicts of interest were disclosed by the other authors.

Authors' Contributions

Conception and design: S.K. Knutson, T.J. Wigle, J.J. Smith, R. Chesworth, R.A. Copeland, V.M. Richon, T. Uenaka, R.M. Pollock, K.W. Kuntz, A. Yokoi, H. Keilhack

Development of methodology: S.K. Knutson, N. Kumar, C.R. Klaus, A. Raimondi, M. Porter-Scott

Acquisition of data (provided animals, acquired and managed patients, provided facilities, etc.): S.K. Knutson, S. Kawano, N.M. Warholic, K.-C. Huang, G. Kuznetsov, N. Kumar, T.J. Wigle, C.J. Allain, A. Raimondi, A. Yokoi

Analysis and interpretation of data (e.g., statistical analysis, biostatistics, computational analysis): S.K. Knutson, S. Kawano, Y. Minoshima, N.M. Warholic, K.-C. Huang, Y. Xiao, T. Kadowaki, M. Uesugi, G. Kuznetsov, T.J. Wigle, C.J. Allain, A. Raimondi, N.J. Waters, J.J. Smith, M. Porter-Scott, R.A. Copeland, V.M. Richon, K.W. Kuntz, H. Keilhack

Writing, review, and/or revision of the manuscript: S.K. Knutson, S. Kawano, K.-C. Huang, Y. Xiao, N.J. Waters, J.J. Smith, R. Chesworth, M.P. Moyer, R.A. Copeland, V.M. Richon, R.M. Pollock, K.W. Kuntz, A. Yokoi, H. Keilhack

Administrative, technical, or material support (i.e., reporting or organizing data, constructing databases): S.K. Knutson, C.J. Allain, H. Keilhack

Study supervision: S.K. Knutson, R.A. Copeland, T. Uenaka, H. Keilhack

Grant Support

This work was funded by Eisai through collaboration between Epizyme and Eisai.

The costs of publication of this article were defrayed in part by the payment of page charges. This article must therefore be hereby marked *advertisement* in accordance with 18 U.S.C. Section 1734 solely to indicate this fact.

Received September 16, 2013; revised December 19, 2013; accepted January 12, 2014; published OnlineFirst February 21, 2014.

References

1. Badeaux AI, Shi Y. Emerging roles for chromatin as a signal integration and storage platform. Nat Rev Mol Cell Biol 2013;14:211–24.
2. Copeland RA, Solomon ME, Richon VM. Protein methyltransferases as a target class for drug discovery. Nat Rev Drug Discov 2009;8:724–32.
3. Copeland RA, Moyer MP, Richon VM. Targeting genetic alterations in protein methyltransferases for personalized cancer therapeutics. Oncogene 2013;32:939–46.
4. Margueron R, Reinberg D. The polycomb complex PRC2 and its mark in life. Nature 2011;469:343–9.
5. O'Meara MM, Simon JA. Inner workings and regulatory inputs that control polycomb repressive complex 2. Chromosoma 2012;121:221–34.
6. Chase A, Cross NC. Aberrations of EZH2 in cancer. Clin Cancer Res 2011;17:2613–8.
7. Lohr JG, Stojanov P, Lawrence MS, Auclair D, Chapuy B, Sougnez C, et al. Discovery and prioritization of somatic mutations in diffuse large B-cell lymphoma (DLBCL) by whole-exome sequencing. Proc Natl Acad Sci U S A 2012;109:3879–84.
8. Morin RD, Johnson NA, Severson TM, Mungall AJ, An J, Goya R, et al. Somatic mutations altering EZH2 (Tyr641) in follicular and diffuse large B-cell lymphomas of germinal-center origin. Nat Genet 2010;42:181–5.
9. Morin RD, Mendez-Lago M, Mungall AJ, Goya R, Mungall KL, Corbett RD, et al. Frequent mutation of histone-modifying genes in non-Hodgkin lymphoma. Nature 2011;476:298–303.
10. Alizadeh AA, Eisen MB, Davis RE, Ma C, Lossos IS, Rosenwald A, et al. Distinct types of diffuse large B-cell lymphoma identified by gene expression profiling. Nature 2000;403:503–11.
11. Beguelin W, Popovic R, Teater M, Jiang Y, Bunting KL, Rosen M, et al. EZH2 is required for germinal center formation and somatic EZH2 mutations promote lymphoid transformation. Cancer Cell 2013;23:677–92.
12. Majer CR, Jin L, Scott MP, Knutson SK, Kuntz KW, Keilhack H, et al. A687V EZH2 is a gain-of-function mutation found in lymphoma patients. FEBS Lett 2012;586:3448–51.
13. McCabe MT, Graves AP, Ganji G, Diaz E, Halsey WS, Jiang Y, et al. Mutation of A677 in histone methyltransferase EZH2 in human B-cell

lymphoma promotes hypertrimethylation of histone H3 on lysine 27 (H3K27). Proc Natl Acad Sci 2012;109:2989–94.
14. Sneeringer CJ, Scott MP, Kuntz KW, Knutson SK, Pollock RM, Richon VM, et al. Coordinated activities of wild-type plus mutant EZH2 drive tumor-associated hypertrimethylation of lysine 27 on histone H3 (H3K27) in human B-cell lymphomas. Proc Natl Acad Sci 2010;107: 20980–5.
15. Wigle TJ, Knutson SK, Jin L, Kuntz KW, Pollock RM, Richon VM, et al. The Y641C mutation of EZH2 alters substrate specificity for histone H3 lysine 27 methylation states. FEBS Lett 2011;585: 3011–4.
16. Yap DB, Chu J, Berg T, Schapira M, Cheng SW, Moradian A, et al. Somatic mutations at EZH2 Y641 act dominantly through a mechanism of selectively altered PRC2 catalytic activity, to increase H3K27 trimethylation. Blood 2011;117:2451–9.
17. Knutson SK, Wigle TJ, Warholic NM, Sneeringer CJ, Allain CJ, Klaus CR, et al. A selective inhibitor of EZH2 blocks H3K27 methylation and kills mutant lymphoma cells. Nat Chem Biol 2012;8:890–6.
18. Konze KD, Ma A, Li F, Barsyte-Lovejoy D, Parton T, Macnevin CJ, et al. An orally bioavailable chemical probe of the lysine methyltransferases EZH2 and EZH1. ACS Chem Biol 2013;8:1324–34.
19. McCabe MT, Ott HM, Ganji G, Korenchuk S, Thompson C, Van Aller GS, et al. EZH2 inhibition as a therapeutic strategy for lymphoma with EZH2-activating mutations. Nature 2012;492:108–12.
20. Qi W, Chan H, Teng L, Li L, Chuai S, Zhang R, et al. Selective inhibition of Ezh2 by a small molecule inhibitor blocks tumor cells proliferation. Proc Natl Acad Sci U S A 2012;109:21360–5.
21. Knutson SK, Warholic NM, Wigle TJ, Klaus CR, Allain CJ, Raimondi A, et al. Durable tumor regression in genetically altered malignant rhabdoid tumors by inhibition of methyltransferase EZH2. Proc Natl Acad Sci U S A 2013;110:7922–7.
22. Ben-Porath I, Thomson MW, Carey VJ, Ge R, Bell GW, Regev A, et al. An embryonic stem cell-like gene expression signature in poorly differentiated aggressive human tumors. Nat Genet 2008;40:499–507.
23. Velichutina I, Shaknovich R, Geng H, Johnson NA, Gascoyne RD, Melnick AM, et al. EZH2-mediated epigenetic silencing in germinal center B cells contributes to proliferation and lymphomagenesis. Blood 2010;116:5247–55.
24. Simon R, Roychowdhury S. Implementing personalized cancer genomics in clinical trials. Nat Rev Drug Discov 2013;12:358–69.
25. Vogelstein B, Papadopoulos N, Velculescu VE, Zhou S, Diaz LA Jr., Kinzler KW. Cancer genome landscapes. Science 2013;339:1546–58.
26. Sandoval J, Esteller M. Cancer epigenomics: beyond genomics. Curr Opin Genet Dev 2012;22:50–5.
27. Timp W, Feinberg AP. Cancer as a dysregulated epigenome allowing cellular growth advantage at the expense of the host. Nat Rev Cancer 2013;13:497–510.
28. Richon VM, Johnston D, Sneeringer CJ, Jin L, Majer CR, Elliston K, et al. Chemogenetic analysis of human protein methyltransferases. Chem Biol Drug Des 2011;78:199–210.
29. Melnick A. Epigenetic therapy leaps ahead with specific targeting of EZH2. Cancer Cell 2012;22:569–70.
30. Kim E, Kim M, Woo DH, Shin Y, Shin J, Chang N, et al. Phosphorylation of EZH2 activates STAT3 signaling via STAT3 methylation and promotes tumorigenicity of glioblastoma stem-like cells. Cancer Cell 2013;23:839–52.
31. Xu K, Wu ZJ, Groner AC, He HH, Cai C, Lis RT, et al. EZH2 oncogenic activity in castration-resistant prostate cancer cells is polycomb-independent. Science 2012;338:1465–9.
32. Bracken AP, Pasini D, Capra M, Prosperini E, Colli E, Helin K. EZH2 is downstream of the pRB-E2F pathway, essential for proliferation and amplified in cancer. EMBO J 2003;22:5323–35.